Reservoir quality prediction of deep-water Oligocene sandstones from the west Niger Delta by integrated petrological, petrophysical and basin modelling

O. K. CHUDI*, HELEN LEWIS, D. A. V. STOW & J. O. BUCKMAN
Institute of Petroleum Engineering, Heriot-Watt University, EH14 4AS Edinburgh, UK
*Correspondence: obinna.chudi@pet.hw.ac.uk

Abstract: Petroleum exploration and production in the region of the Niger Delta to date has mainly focused on the onshore, deltaic and offshore deep-water Miocene successions. Although Miocene turbidites have been the principal deep-water target, deeper-lying Oligocene sandstones are now being considered for exploration. This study targets an area beneath the Niger Basin slope at a present-day water depth of 800–1500 m. Within this study area, the Miocene to Recent sands above a burial depth of 3600 m show very good reservoir quality with porosities as high as 35% and permeabilities in the Darcy range. The aim of this study is to predict the reservoir quality and properties of the Oligocene sandstones below 3800 m using basin modelling to predict conditions where quartz cementation will take place and quartz cementation models to predict the amount of cementation and hence the potential porosity loss. Modelling results show that the Oligocene sandstones have been exposed to conditions favourable for quartz precipitation, but that less than 14% of the original porosity will have been occluded by quartz cement. These results are in agreement with elemental analysis from both petrophysical and petrological observation of thin sections. Although the deeper-lying Oligocene sandstones are likely to have reduced reservoir quality due to the presence of quartz overgrowth cementation, it appears likely that the volume of cement is relatively low and the Oligocene succession should be considered a viable play.

The Miocene clastic succession of the prolific Niger Delta province has been a major target for hydrocarbon exploration since the 1950s and is responsible for hosting most of the discoveries in both the onshore and offshore parts of the delta system (Doust & Omatsola 1990; Saugy & Eyer 2003; Reijers 2011). In part, this is due to the excellent porosity and permeability characteristics of the poorly consolidated reservoir sands (Weber 1971). Porosities of up to 35% and permeabilities of more than 3 D have been reported from well logs and cores across producing fields in the delta region. There has been no or minimal cementation and very little precipitation of authigenic minerals, which are dominated by quartz overgrowths, within the primary porosity. The reservoir quality of the Miocene interval has only undergone a low level of degradation.

As the quest for further hydrocarbon reserves increases, exploration and production is gradually moving from the shallow and more easily identifiable reservoirs of the Miocene to deeper-lying Oligocene plays that have been exposed to higher temperatures and hence physical and chemical conditions that are more conducive to quartz precipitation. The aim of this study is to estimate the degree of quartz cementation in unexplored, deeply buried, Oligocene deep-water clastic sediments of the basin slope of the Niger Delta region. We apply an integration and cross-comparison of basin modelling, cementation modelling, petrological analysis and petrophysical multimineral elemental analysis.

The Niger Delta has been the centre of attraction for hydrocarbon exploration and production on the continental margin of West Africa for over four decades (Haack et al. 2000) and has consequently has thoroughly studied (Short & Stauble 1967; Weber 1971; Whiteman 1982; Ejedawe et al. 1984; Damuth 1994; Haack et al. 2000). The delta is situated

in the Gulf of Guinea and covers an area of approximately 140 000 km2 with a maximum clastic sediment thickness of about 12 km at the basin centre (Damuth 1994). The study area is located in the translational tectonic province in the mid-slope of the Niger Delta deep-water system (Fig. 1). The proven reservoir intervals are Miocene channel sands with porosity values greater than 30% and permeability in the Darcy range. Of over 30 wells drilled in the study area only one well penetrated the top of the Oligocene succession, which is the primary interval of interest for this study.

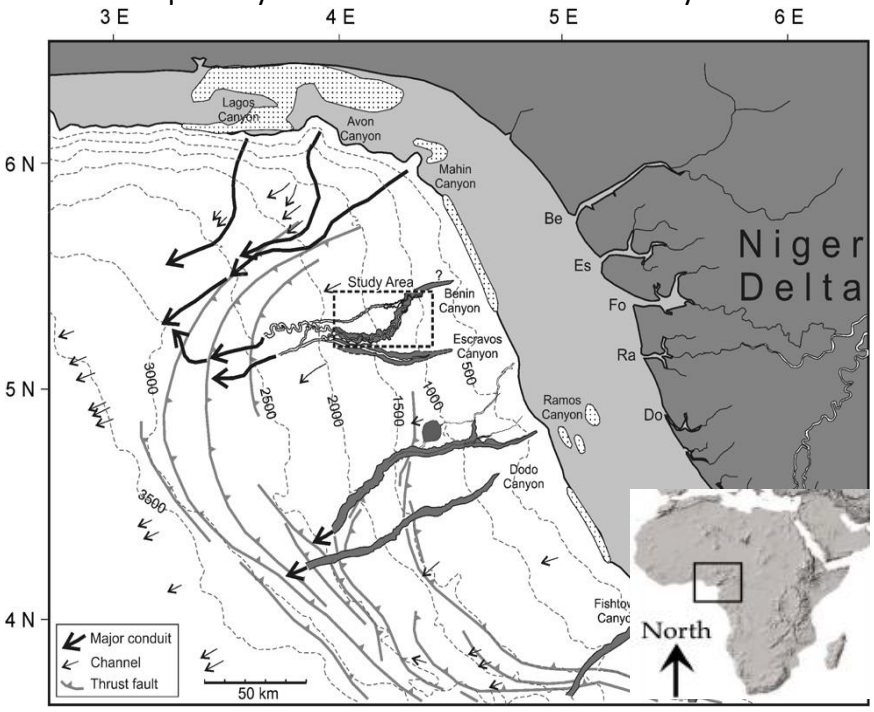

Fig. 1. Regional location map showing the western Niger Delta and study area. Adapted from (Deptuck *et al*. 2007).

Generally reservoir rock quality is controlled by variables such as the grain size, initial depositional porosity, mechanical compaction, chemical compaction, mineralogy and volume of pore filling cement (Worden & Morad 2009). The diagenetic changes that influence reservoir properties, such as porosity and permeability, are affected by an interplay of these factors under conditions of increased effective stress, temperature and burial (Taylor et al. 2010). The regional geothermal gradient of the whole Niger Delta region ranges from 1.3 to 1.8°C per 100 m in the centre of the basin and increases up-dip and northwards to about 2.7–5.5°C per 100 m (Nwachukwu 1976; Doust & Omatsola 1990). These controlling variables have influenced the strategy and the technique adopted herein for petrophysical evaluation across fields within the delta system.

The accurate prediction of sandstone reservoir quality is a key challenge for hydrocarbon exploration and production. A good understanding of reservoir quality is required throughout the entire lifecycle of a reservoir; from exploration (where it is required for the estimation of the initial hydrocarbon reserves) to the appraisal and development stages where the porosity and permeability distribution in a reservoir are necessary for well-placement optimization and to estimate economic cut-off limits that control estimates of hydrocarbon pore volumes, recoverable reserves and production rates (Sneider 1990). A fundamental control on the quality of a sandstone reservoir, especially for siliciclastic

systems, is quartz cementation. This is controlled by the temperature, pressure (effective stress) and surface area of the quartz substrate, which is itself a function of the grain size, abundance of grain coatings and quartz clast abundance (Walderhaug 2000; Worden & Morad 2009).

We present a synthesis of petrological, petrophysical and basin modelling studies to characterize the poorly understood potential Oligocene reservoirs of the mid-slope, deep-water part of the Niger Delta Basin. The focus of this work is to better understand and investigate the reservoir potential of the Oligocene interval buried below 3800 m, and most importantly its diagenetic history, using a novel integrated methodology. The burial, temperature and pressure histories have been considered, in addition to their key controls on quartz cementation. Petrological analysis of thin sections and polished block samples of the hydrocarbon-charged shallower Miocene samples were studied and inferences made to predict the mineralogy of the uncored Oligocene interval that was penetrated by a single well (A1). The petrological study was integrated into multimineral petrophysical study to predict the composition of the sandstones from well log responses. We further consider the applicability of this approach and these findings to analogous subsurface systems around the world.

Geological setting

Rifting and break-up of Africa from South America in this region initiated in the Early Cretaceous, with a triple junction located approximately beneath the region that is now the Niger Delta. By the Late Cretaceous, spreading of the Atlantic was underway along the southern and western arms of this tri-rift systems, whereas the NE arm, the Benue Trough, became a failed rift system. By the Palaeocene, the Niger Delta region had begun to receive significant sediment input from the land. Through the Palaeocene and Eocene there were probably at least three principle depocentres linked to marked sediment progradation over the subsiding continental– oceanic lithospheric transition zone. By the Oligocene, these three depocentres had merged into the single major arcuate depocentre that is now the Niger Delta. The increased sediment load on a cooling and subsiding basement further enhanced subsidence in the region. Since this time the delta has prograded in a generally SW direction creating a series of major depositional belts that represent the most active portion of the delta at each stage of development. The principal sediment provenance for the western delta region has been the Benue–Niger drainage system, whereas the eastern delta region was sourced from the Cross River system. The present day Niger Delta complex takes the form of a constructive arcuate delta, with mud diapirism beneath the slope playing a major role in controlling sediment distribution (Whiteman 1982).

Lithostratigraphy

The Tertiary Niger Delta complex comprises a tripartite lithostratigraphic sequence: the Benin, Agbada and Akata formations (Fig. 2). Each of these formations represents deposition in one of three main sedimentary environments: continental, transitional and marine, respectively. These depositional environments are arranged laterally from proximal to distal and, as a result of marked progradation, they also stack up vertically with the continental

Benin Formation overlying the transitional (marginal marine) Agbada Formation, which in turn overlies the marine/deep-marine Akata Formation. We describe each briefly below from proximal to distal.

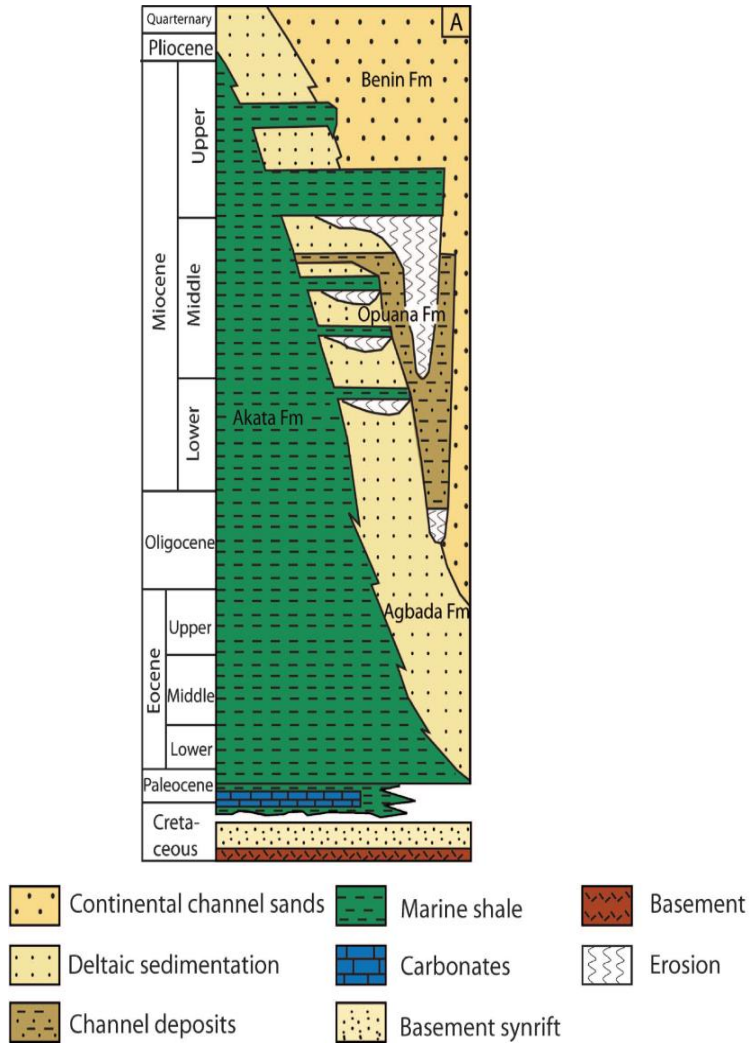

Fig. 2. Stratigraphy of the Niger Delta (after Corredor *et al.* 2005).

The proximal continental environments comprise sediments of the upper delta plain and fluvial feeder system and are represented by predominantly sandy lithologies. The sediments are poorly sorted, granular and pebbly, coarse to very fine grained. They are assigned to the Benin Formation, which occurs wholly onshore at the present day, but also extends a short distance offshore in the subsurface (Short & Stauble 1967). The known age of the Benin Formation is from Oligocene to Recent although, presumably, an equivalent lithostratigraphic unit also acted as sediment source for the older delta deposits.
The Benin Formation generally exhibits poor reservoir quality and so is not an effective reservoir target.

The transitional, marginal marine environment comprises interbedded sandstones and shales assigned to the Agbada Formation. The shale units are more prominent with depth, becoming progressively thicker than the intercalated sandstone units; this reflects the seaward advance of the delta system through time (Whiteman 1982). The sandstones

constitute the principle reservoir units in the Niger Delta Basin, exhibiting excellent reservoir quality. They were most likely charged through large-scale open growth faults that were connected to adjacent kitchen areas. The Agbada Formation extends throughout the Niger Delta region and represents deposition in both lower delta plain and marginal marine to continental shelf environments.

The interplay between subsidence and sediment supply, and the relative change in sea-level, has driven transgressive and regressive cycles that are responsible for alternating sandstones and shale sequences (Doust & Omatsola 1990). The known age of the Agbada Formation ranges from Eocene to Recent.

The distal and fully marine environments are represented by a more mud-rich succession known as the Akata Formation. The marine shales of this sequence range from Palaeocene to Recent in age, and are mainly characterized by hemipelagic slope sediments intercalated with turbidite sandstones. Regional studies and experimental analysis suggest that the Akata Formation provides the principal hydrocarbon source rock for the Niger Delta province (Evamy et al. 1978; Lambert-Aikhionbare & Ibe 1984; Tuttle et al. 1999). The Akata shales are extensive across the whole region, whereas the turbidite sands are more localized as deep-water channel and lobe deposits.

These channel-lobe turbidites provide the principal deepwater reservoirs of Miocene age as well as the proposed Oligocene reservoir targets. Similar features are recognized through the Pliocene section as well as across the present day Niger Delta slope. Certainly there is no evidence either from seismic interpretation or from borehole studies to suggest any significant change in sediment provenance or depositional processes between the Oligocene and Miocene systems. We are therefore confident in using what we know of the Miocene reservoirs as a template for understanding the Oligocene.

Tectonics and structure

The end of Atlantic rifting in the Late Cretaceous gave way to gravity-driven tectonism as the primary deformational process affecting delta development. Owing to a rapidly prograding delta, low permeability, fine-grained, pro-delta muds became overpressured and formed mud diapirs as a response (Whiteman 1982). Diapirism began in the Miocene and is still taking place today both at the delta front and extending further into the deep-water basin. The growth of the diapirs resulted in the development of section and flatten onto a decollement surface at the top of the hemipelagic muds. The overall structural trend is oriented in a NW–SE direction (Haack et al. 2000). Three structural provinces generally define the delta (Fig. 3): (a) an extensional province that extends from onshore to the outer shelf region, marked by large-scale listric growth faults; (b) a translational province across the upper and middle slope, dominated by mud diapirs and folds; and (c) a compressional province in the lower slope region, triggered by tectonic-scale downslope movement of sediment due to gravity gliding, which leads to toe thrust features and a marked fold and thrust belt (Bilotti&Shaw 2005; Corredor et al. 2005; Deptuck et al. 2007).

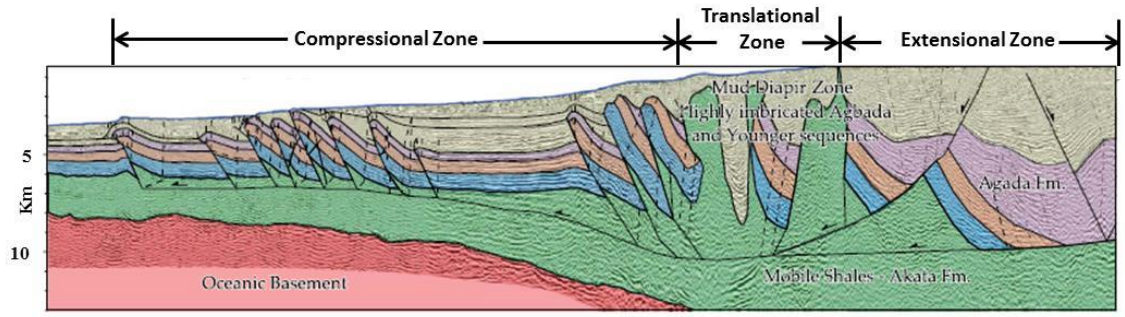

Fig. 3. Regional cross section showing the three structural provinces of the Niger Delta (modified from Corridor *et al.* 2005).

Methods

Petrography

Petrological analyses were conducted on 17 samples acquired from four wells in the study area. The cored samples were taken from the Miocene interval; from the Middle Miocene at a depth of approximately 2470 m and from the lower Miocene at 3450 m. Samples taken from depths shallower than 3000 m were unconsolidated sands. All samples were made into thin sections and polished blocks as appropriate. The samples were dried at 38°C and vacuum-impregnated with epoxy resin. Ultraviolet glue was further applied to mount cover slips. For the purpose of SEM studies, samples were also made into polished blocks by drying at 38°C and placing in a 25–30 mm diameter mould. The granular samples were filled with epoxy resin, mixed by stirring and placed under vacuum to remove air bubbles.

Techniques used included light optical microscopy and scanning electron microscopy (SEM) using back-scattered electron imaging (BSE) and cathodoluminescence (CL) analysis. Samples were examined uncoated and in low-vacuum mode, using a Quanta 650 FEG SEM and XL30 LaB6 ESEM.

Optical microscopy was used for mineralogical identification, and where the optical identification of quartz overgrowths was difficult SEM was used. CL analyses were carried out on the SEM with a Centaurus CL detector. A combined BSE and CL analysis was undertaken using a similar method to that outlined by Evans et al. (1994), which involves the analysis of pairs of BSE and CL images from polished block samples. A set of 13 samples were selected for this analysis. CL is particularly useful in distinguishing detrital quartz grains from syntaxial quartz overgrowths.

Petrological analysis was carried out over the Middle and Lower Miocene intervals to investigate the probable presence of microcrystalline quartz or chlorite rims, as they can impede the nucleation of quartz overgrowth if present (Bloch et al. 2002; Marchand et al. 2002; Taylor et al. 2010).

Petrophysical analysis

Wireline log data from four wells within the study area were analysed to characterize the porosity and permeability of the reservoir zones penetrated. Of the four wells studied only one well penetrated the Oligocene interval. The density log was used to calculate porosity

and these values were calibrated against core porosity where available. Permeability was estimated using the neural network technique, where sets of input logs (gamma ray, sonic, density and neutron logs) were trained to recognize the core-derived, stress-corrected air permeability, acquired from routine core analysis (Sonde et al. 2011).

A multimineral model based on petrophysical elemental analysis (ELAN) of open-hole logs was used to compute the volume of mineralogical components within the intervals of interest. ELAN uses log curves and the response parameters of the tools to compute the volumetric constituents of the minerals and fluid in the formation. This method derives the relative quantities, or relative volumes, of the mineral components that would most probably produce the set of measurements recorded by the logging instruments. The three-way relationship between tools (T), response parameters (R) and formation component volume (V) is shown in Figure 4.

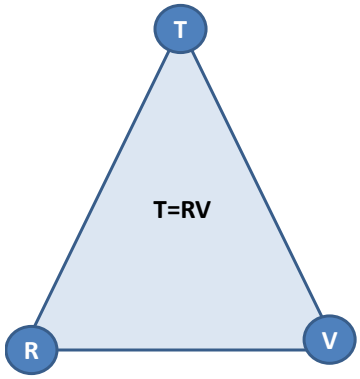

Fig. 4. Schematic illustration of ELAN. T represents the tool vector which in this case is the input log data (gamma ray, resistivity, neutron, density, and calculated porosity logs) and R is the response matrix which is a pre-defined value for the reading each tool would give for 100% of each formation component. R values were determined based on the known mineralogical responses to the physics of the different tools (Reeder *et al*., 2013) as defined using the Schlumberger Techlog software package. V is the volume vector which is the volume of each formation components.

Given the data represented by any two corners of the triangle (Fig. 4), the third can be determined. In this study, T and R are used to compute V. For quality control, forward-modelling of R and V are used to reconstruct T – the input logs. The reconstructed logs are compared against the input data to determine the quality of the volume results. Four principal minerals (quartz, feldspar, zircon and kaolinite) were modelled in ELAN based on their abundances determined in the petrographic study.

Basin modelling and diagenetic evolution.
Since the early 1980s basin modelling has been used to study the burial and thermal evolution of a basin; particularly in relation to petroleum generation, expulsion, migration, accumulation and preservation (Welte & Yalcin 1988; Wygrala 1988; Talc¸in 1991; Hermanrud 1993; Underdown & Redfern 2008). Basin modelling has also been used by some authors to study diagenetic evolution and to infer its impact on reservoir quality, particularly on porosity (Sombra & Chang 1997; Walderhaug 2000) by attaching a

calculation of the appropriate chemical reactions to the states generated by the basin model at different burial positions. Siever (1983) first associated chemical reaction calculations with fluid type and conditions, with stress and fluid pressure states and with temperature, permitting an estimate of the transformation of organic matter to petroleum and also of quartz precipitation from a silica-rich fluid. Before this study by Siever (1983), the compaction models proposed by Athy (1930) were used to calculate porosity evolution, using the degree of sediment compaction, but these relationships were sufficient to calculate the effect of porosity changes due to cementation or dissolution. Starting with Siever (1983), models can relate the calculated (or otherwise derived) basin history to temperature and to appropriate diagenetic reactions. However basin-modelling studies are certainly not the only method available to estimate palaeothermal and palaeochemical states. For example, palaeotemperatures have been regularly inferred from the petrographic study of fluid inclusions, and particularly from chemical composition and isotopic signatures. Sombra & Chang (1997) follow this approach, using time–depth indices (TDI) to quantify the influence of burial history on the evolution of sandstone porosity.

Basin modelling. The 2D basin model uses the transect shown in Figure 3, oriented NE–SW and extending over 160 km across the extensional, translational and compressional parts of the Niger Delta Basin (Bilotti & Shaw 2005; Corredor et al. 2005; Deptuck et al. 2007; Fig. 5). A total of seven chronostratigraphic horizons, the Seafloor, Lower Pliocene, Upper Miocene, Mid Miocene, Lower Miocene, Oligocene and Basement were digitized and used in this study. Each of the resulting defined units was assigned suitable lithologies. Where no well control was available, each lithology was initially assumed to be laterally continuous. Other basic requirements for modelling include boundary conditions, calibration data (corrected bottomhole temperature (BHT), vitrinite reflectance, pressure, porosity and present-day hydrocarbon accumulations) and source rock properties, particularly the kinetic parameters that are responsible for the type and amount of generated petroleum. Interpreted faults on the 2D transect were also digitized, with priority given to the faults that are likely to have a significant impact on hydrocarbon migration. The fault selection method used adopted similar criteria to those chosen by Derks et al. (2012).

Quartz cement modelling. In this study the basin modelling tool used is PetroMod V. 2013, which has an additional quartz cementation calculation module based on the Walderhaug quartz cementation model (Walderhaug 2000). This module was well optimized with measured data (corrected BHT, vitrinite reflectance, pressure and porosity). The amount of quartz cementation over the time– depth range represented in the basin model was then calculated. However, Walderhaug (2000) expressed the effect of cementation as a function of the change in quartz surface area whereas PetroMod models cementation as a function of the rate of porosity loss. Equation (1) shows the relationship expressed by the Walderhaug quartz cementation model:

$$A = (1 - C)6\, fV\phi / D\phi_0 \qquad (1)$$

where A is the change in quartz surface area, C is the fraction of the quartz grain surface coated by clay or other substances, f is the volume fraction of quartz clasts, V is the sample volume and D is the average quartz grain diameter. PetroMod uses the cementation

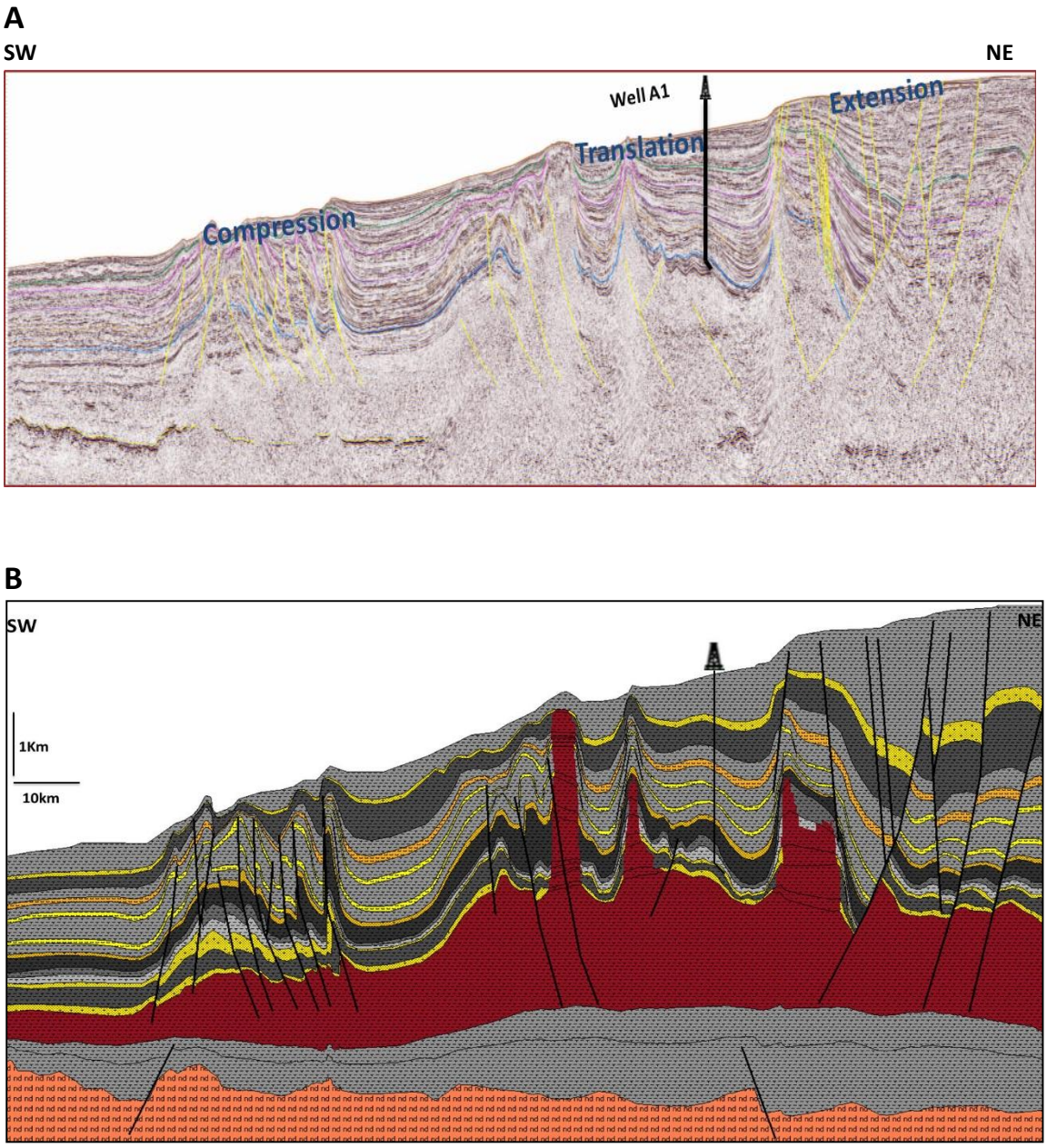

Fig. 5. A) Interpreted regional 2D transect across the 3 structural provinces; B) Digitized 2D transect

equation shown in equation (2). Both cementation modelling algorithms vary with assigned detrital mineralogy, quartz grain size, quartz grain coating abundance, temperature and A. The porosity loss rate due to quartz cementation that has been adopted in PetroMod is therefore expressed as:

$$\frac{\delta\phi cc}{\delta t} = \frac{m}{\rho}\frac{(1-C)6f}{D}\frac{\phi}{\phi_o}Ae^{-Eo/RT} \qquad (2)$$

where C is the quartz grain coating factor, f is the quartz grain volume fraction, D is the average quartz grain diameter, A and E_o are respectively the frequency factor and activation

energy of quartz precipitation. m represents the mole-mass and ρ the density of quartz (Walderhaug 1994).

The average grainsize and quartz grain volume fraction used in the quartz cementation calculations were based on the results of the petrological study. A dominant grain size range of 125–500 mm is seen in the Miocene. No core has yet been taken from the Oligocene interval. So, in the absence of any grain size measurements, it was assumed that the Oligocene reservoirs in the study area, which are below 3800 m, would have a similar grain size as the Lower Miocene reservoir at 3450 m, the deepest cored section available to this study.

The PetroMod calculation assumes that quartz is sourced by stylolitization. In addition, it is also assumed that the precipitation phase of the overall quartz dissolution, transportation and precipitation process is the slowest and hence acts as the rate controlling step in the entire process (Walderhaug 2000).

By implementing the Walderhaug quartz cementation model as part of the simulation, the percentage of the pore space that is occluded by cement was estimated. The results show that cement volume tends to increase both with depth and with the landward and up-dip distance along the regional transect (Fig. 6) as water column thickness decreases and mean overburden increases. Little or no cement is predicted above 3000 m but cementation starts

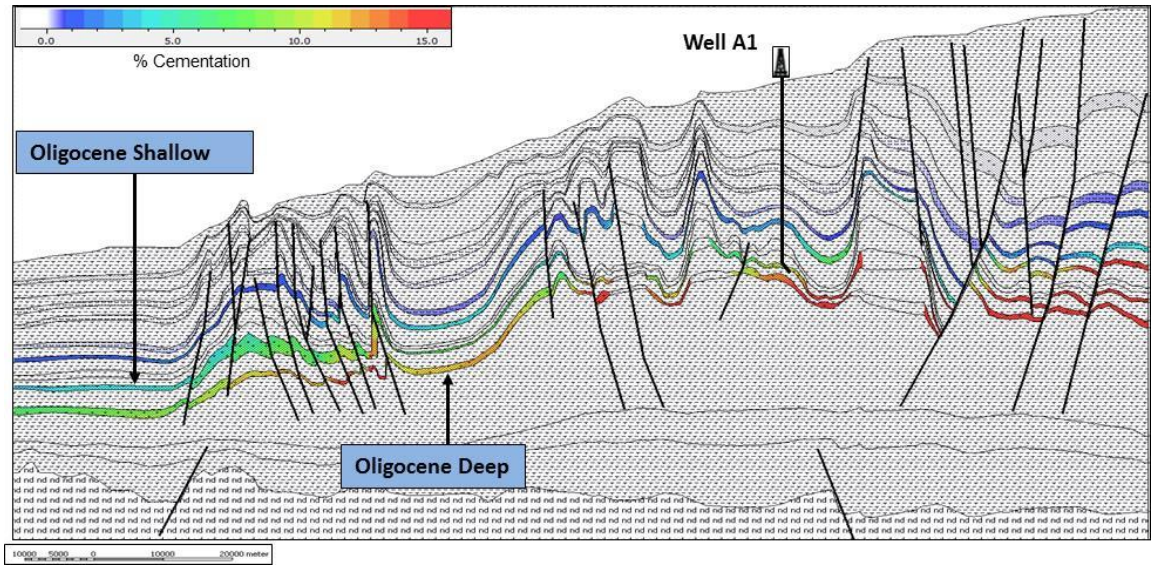

Fig. 6. Overlay of predicted quartz cement on 2D transect. Colour spectrum show increase in cement volume from blue to red. In the vicinity of well A1 cement volume increase with depth from Miocene to Oligocene.

to develop from about 3450 m depth within the Lower Miocene reservoirs with less than 5% of the pore space now containing quartz cement. The cement volume increases steadily with depth into the potential Oligocene reservoirs with values of close to 14% of pre-cementation pore space. The minor quartz cement observed from the petrographic study for the Lower Miocene reservoir and the absence of quartz in Middle Miocene agrees with

this modelled result. The modelled result is also displayed as a 1D extraction at the well location from the 2D model with cement volume plotted against depth (Fig. 7).

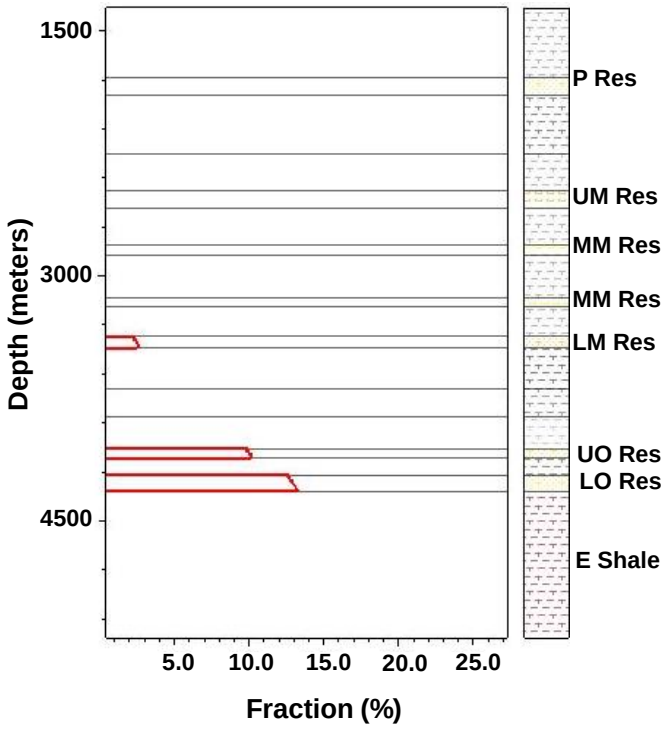

Fig. 7. Fraction of pore space occluded by quartz cement plotted against depth: a 1D extract from the 2D model. (Res =reservoir, P =Pliocene, UM = Upper Miocene, MM = Mid-Miocene, LM = Lower Miocene, UO = Upper Oligocene, LO = Lower Oligocene, E = Eocene).

Results

Miocene sediments

The Miocene reservoirs in the study area are typically composed of loosely consolidated sands that are moderately sorted and display a dominant grain size of medium to fine, although coarser grain sizes also exist. The sands are classed as quartz arenites (according to the classification of McBride 1963) as they are largely composed of quartz with less than 15% feldspar and a minor lithic component (<2%). The excellent quality of the reservoir sands is largely attributed to the unconsolidated nature of the sands with little or no cementation present.

A total of 15.1 m of cores was studied; 12 m across the Middle Miocene and 3.1 m across the Lower Miocene sequence. The Middle Miocene reservoir facies comprise massive, unconsolidated sands that are typical of the Bouma Ta facies, with minor normal grading seen in the sands. High density turbidity current flow is the most likely depositional mechanism. Two facies have been noted in the Lower Miocene: (1) light grey, very fine consolidated massive sands that are moderately to well sorted, representing deposition by high-density turbidity currents, and (2) interlaminated very fine sands and silts that are characterized by millimetre- scale parallel and convolute lamination. Some dark laminations are also noted and are most likely to be mud or organic material. These facies probably represent deposition by dilute turbidity currents. Figure 8 is a schematic of the

sedimentological log of the core section studied, with representative core photographs of facies where samples for petrographic analysis were taken.

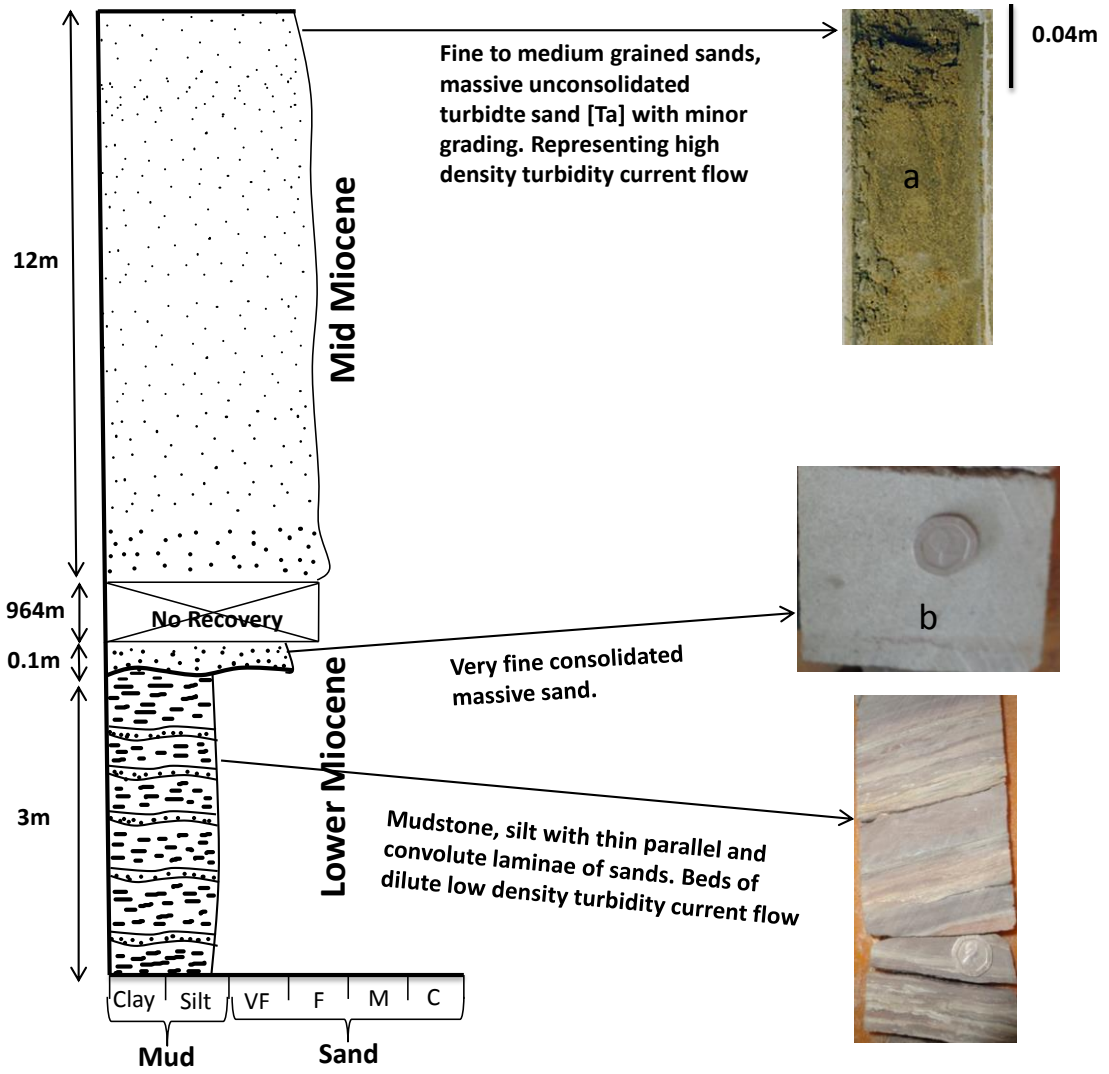

Fig. 8. Sedimentological log of core from well A1 across the Mid Miocene and Lower Miocene sections. Core photos represent typical examples of the lithologies described; petrographic samples were taken from 'a' and 'b'.

Petrological analysis

Detrital mineralogy. The Miocene samples from the three wells examined by optical microscopy are composed dominantly of quartz, comprising up to 85% monocrystalline grains with minor polycrystalline quartz, 10% feldspar and 0–5%lithic fragments of possible igneous and metamorphic origin (Fig. 9). Muscovite and heavy minerals (probably zircon) occur in trace amounts. Heavy minerals are easily recognizable using BSE micrographs as highly luminescent grains, as depicted in Figure 10a, c. Grain size ranges between fine and medium sand (125–500 mm), with sorting from poor to well sorted and grain roundness from subangular to angular.

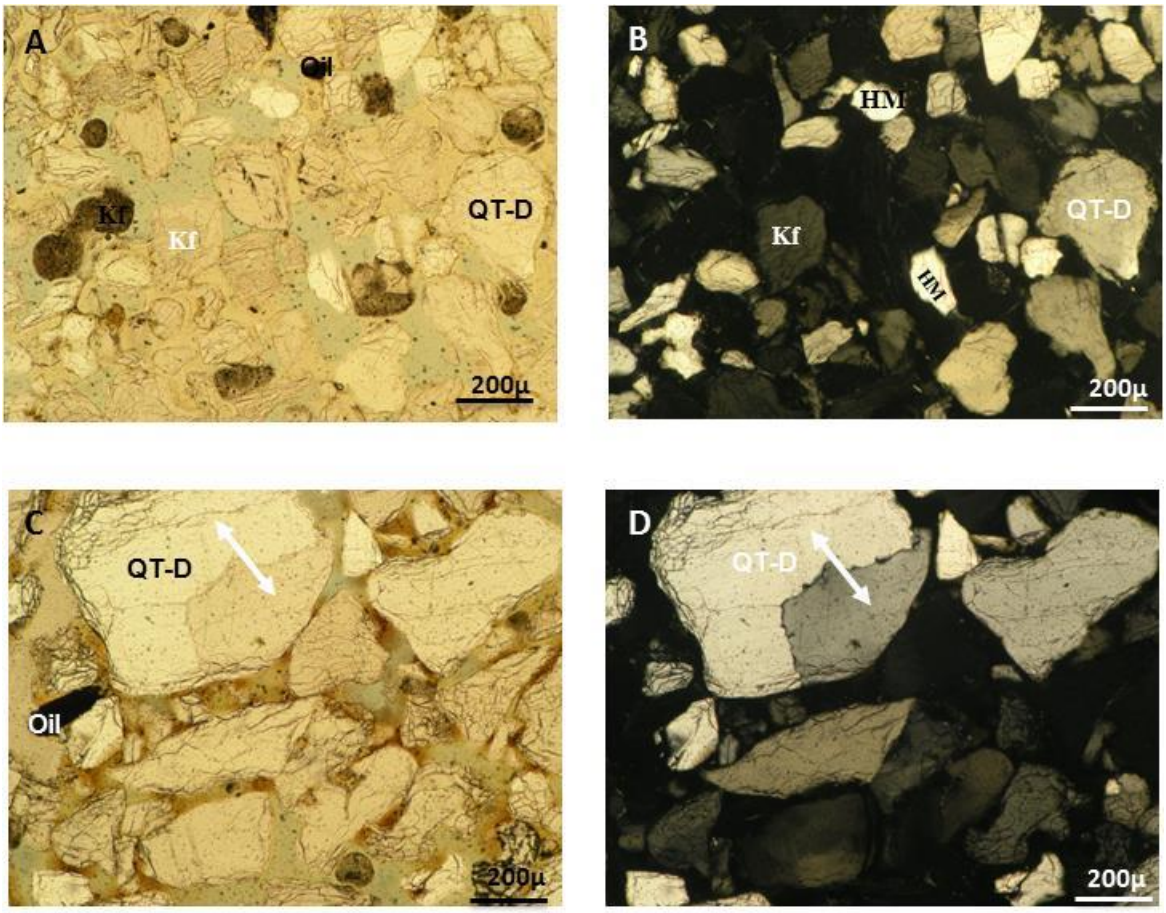

Fig. 9. Photomicrographs in both plane polarised light and cross polars of Mid-Miocene (A, B) and Lower Miocene reservoirs (C, D), (detrital quartz (QT-D), K-feldspar (Kf), polycrystalline (arrows)).

Diagenetic mineralogy

Quartz cement. Quartz cements are rarely observed in thin sections in the Middle Miocene samples located at depths of less than 3000 m. However, thin sections of samples retrieved from the Lower Miocene reservoirs at 3450 m do show some quartz overgrowths. In some cases they occur as euhedral overgrowths protruding into primary pores. The overgrowths range in size from individual small euhedral crystal growths of 3–20 mm to grain-rimming cements of less than 30 mm in thickness. Overgrowths are not widespread but are locally developed around quartz grains. CL and BSE analyses allowed distinction between authigenic and detrital quartz. Authigenic quartz rims are typically less luminescent than their detrital host (Fig. 10d). Topographic secondary electron images also reveal quartz overgrowths with well-defined crystal faces over the surface of the detrital host (Fig. 10e). BSE analyses of the same sample showed no distinction as both detrital and authigenic quartz display the same false colour grey (Fig. 10c).

Grain coating. The SEM analysis of the samples does not reveal the presence of any grain-coating minerals of early origin. The Upper Miocene samples are coated with thick 'dead'/bituminous oil (Fig. 11). The presence of this oil is indicative of biodegradation due to exposure of the Middle Miocene reservoir to temperatures lower than 60^{o}C (Peters et al. 1996).

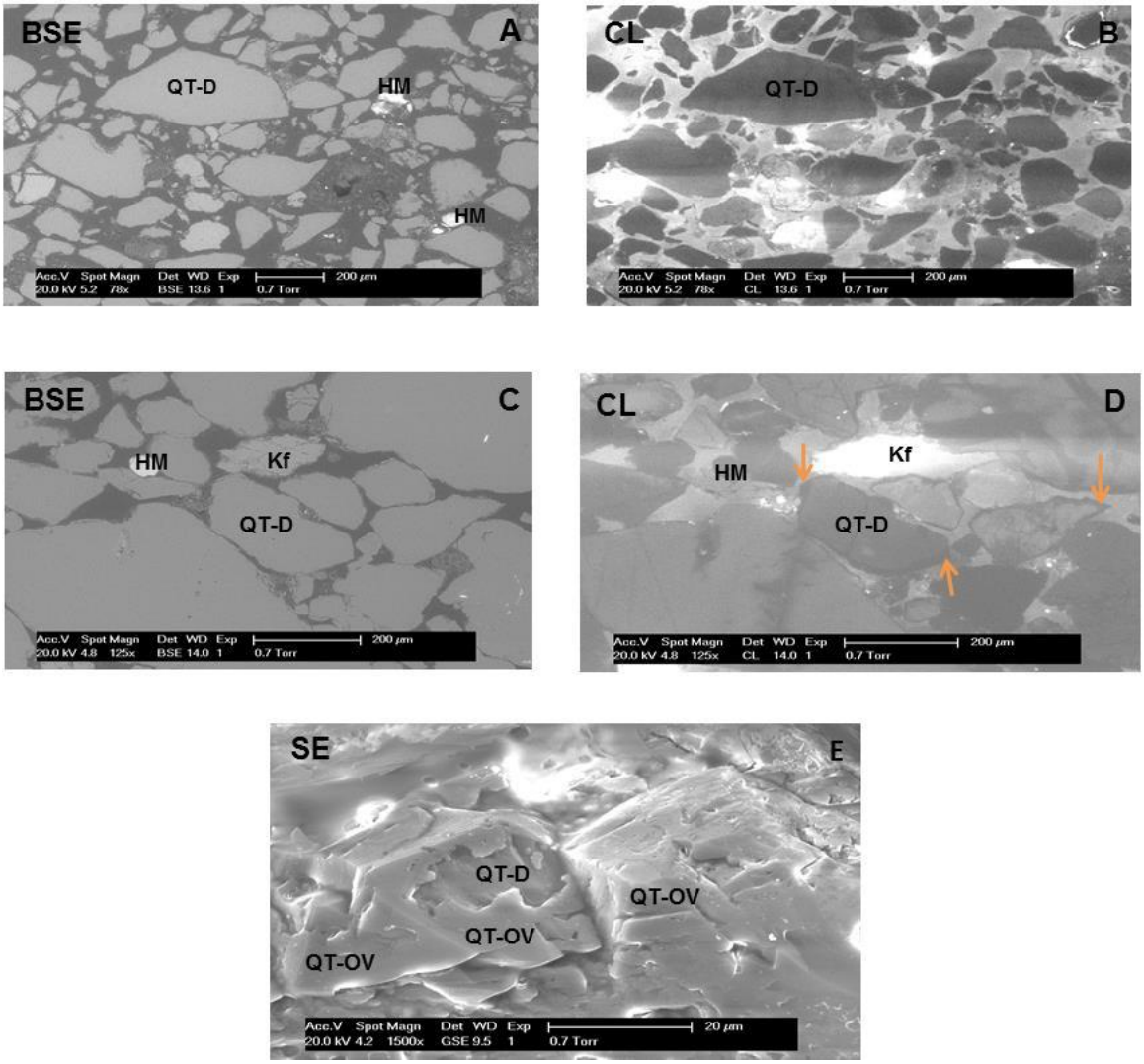

Fig. 10. Upper Miocene polished block samples with no quartz cement seen from both BSE and CL plates (A and B), while overgrowths (indicated by amber arrow) are present in the Lower Miocene samples (C, D and E), (detrital quartz (QT-D), quartz overgrowth (QT-OV), K-feldspar (Kf), heavy mineral (HM)).

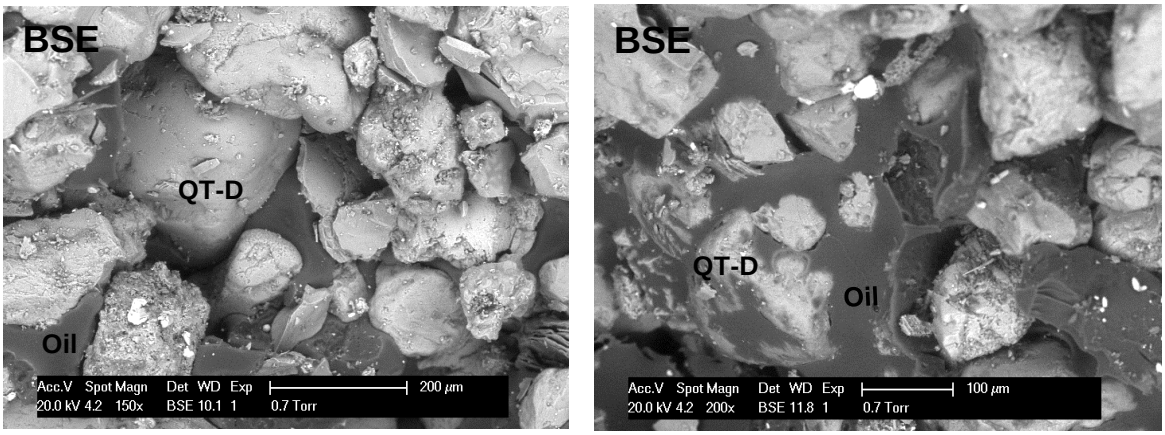

Fig. 11. BSE image of Upper Miocene samples showing quartz grains surrounded by oil.

Clays: SEM examination revealed the presence of kaolinite-type clay in both the Upper Miocene and the Lower Miocene successions. These clays occur as stacked pseudo-hexagonal crystals of euhedral booklets (Fig. 12a–c). In the Lower Miocene succession kaolinite is observed blocking primary intergranular porosity, suggesting that the kaolinite clay developed before the main phase of mechanical compaction (Gier et al. 2008; Fig. 12c).

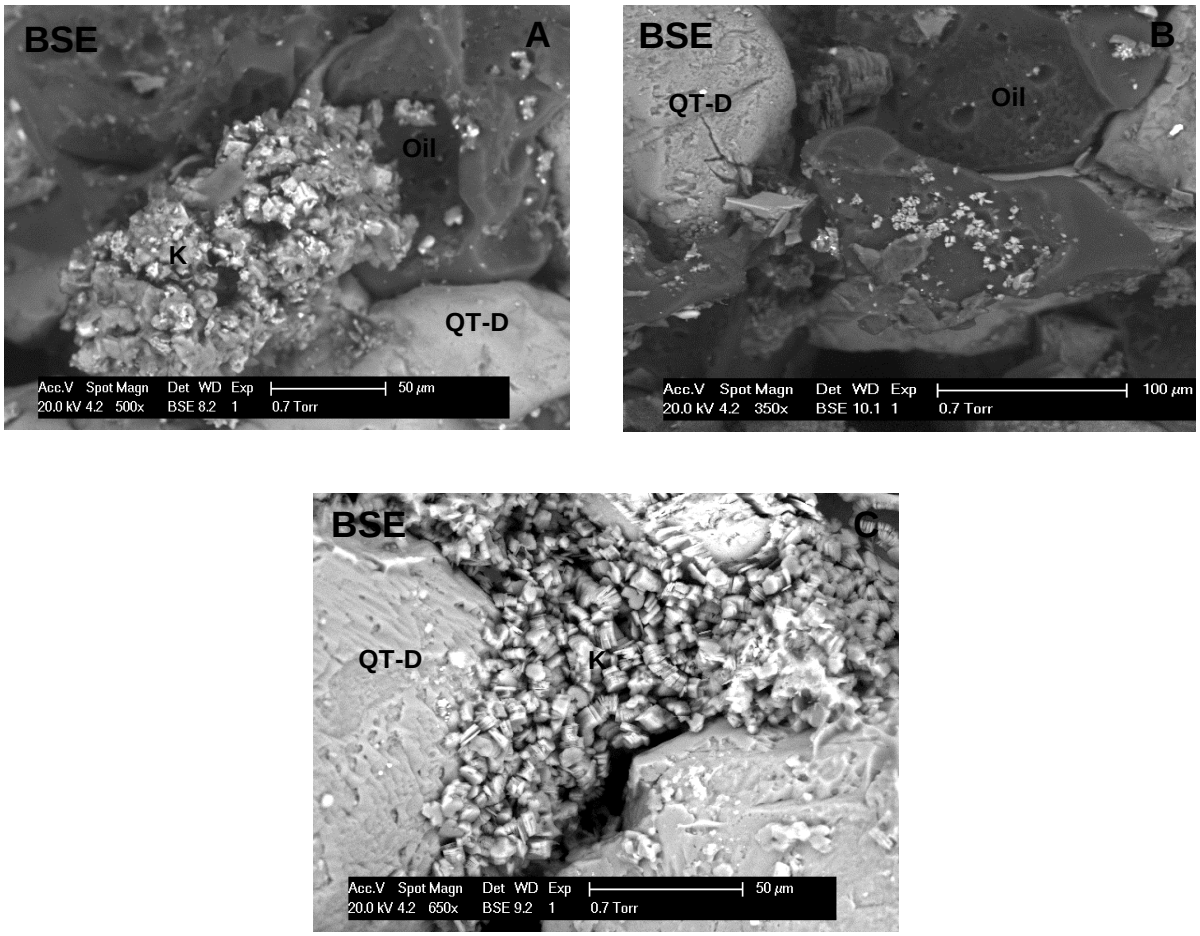

Fig. 12. BSE images of Upper Miocene and Lower Miocene Sandstones. A and B images show authigenic kaolinite surrounded by oil, (C shows pore filling kaolinite crystals: (detrital quartz (QT-D), quartz overgrowth (QT-OV), oil, kaolinite (K)).

Petrophysics

The porosity calculated from wireline log analysis (for example, Fig. 13) decreases with depth as seen from the porosity depth plot of four wells in the study (Fig. 14). Figure 14 also reveals that only the estimated porosities from Well A1 (represented by a triangle), which is the only well that encountered the Oligocene reservoirs, have average porosity values of 20%. The porosity for the Miocene samples generally ranges from 21% to 37% across all of the wells (see Fig. 14).

The results of the multimineral analysis are displayed in Figure 15. Tracks three to seven of Figure 15a show the input logs while the last track shows the multimineral model derived from the open-hole logs. The modelled quartz volume is seen to increase with depth as observed from the cross plot of quartz volume as a fraction of the total reservoir component (mineral, fluid and rock) plotted against depth (Fig. 15b) with two trend lines seen.

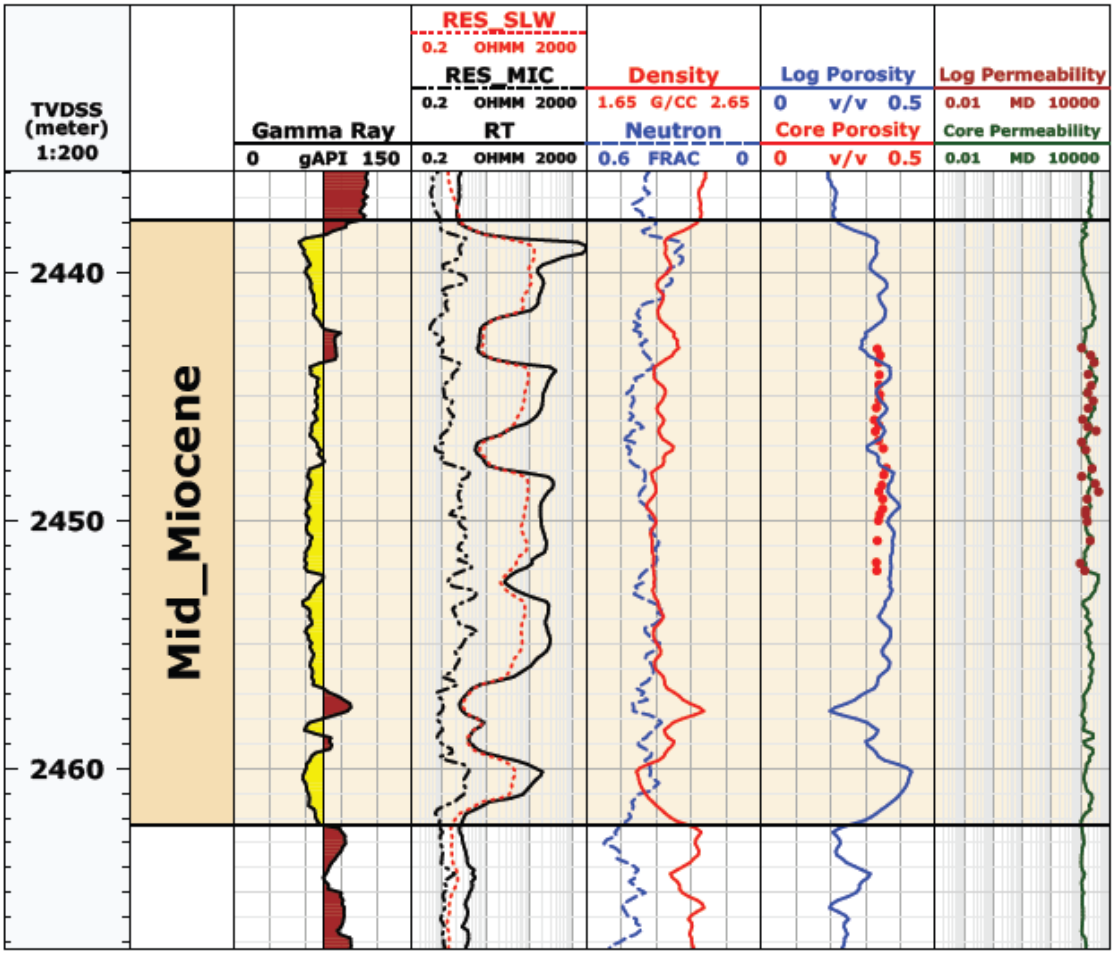

Fig. 10. Petrophysical data log showing modelled porosity calibrated to core porosity (rec dots right but one column) and modelled permeability calibrated against core permeability (red dots rightmost column).

However, it is not possible to verify the proportions of detrital and authigenic quartz from the multimineral model. The first trend line (a) indicates a steady increase in the quartz volume of close to 60% with depth from the Upper Miocene to the Middle Miocene reservoirs. An offset is seen in the second trend (b), representing the quartz volume for the Lower Miocene down to the Oligocene with an estimated quartz volume of close to 80% in the Oligocene reservoir intervals.

Basin modelling

Temperature and pressure history. The thermal history calculated by the 2D basin model shows that the Middle Miocene and younger reservoirs in the study area have never been exposed to temperatures above 60°C (Fig. 16a), which is below the 70–135°C initiation of effective quartz precipitation temperature range (Walderhaug 1994; Bjørkum et al. 1998). On the other hand both the Lower Miocene and the Oligocene intervals are calculated to have reached temperatures above 70°C. The Oligocene has been exposed to temperatures above 70°C from the Early Miocene (19 Ma) to the present (reaching 90°C in the Middle Miocene and 120°C by the Pleistocene, Fig. 16a). In contrast, the Lower Miocene reservoirs encountered temperatures of 70°Cand above from the Early Pliocene, reaching about 80°C

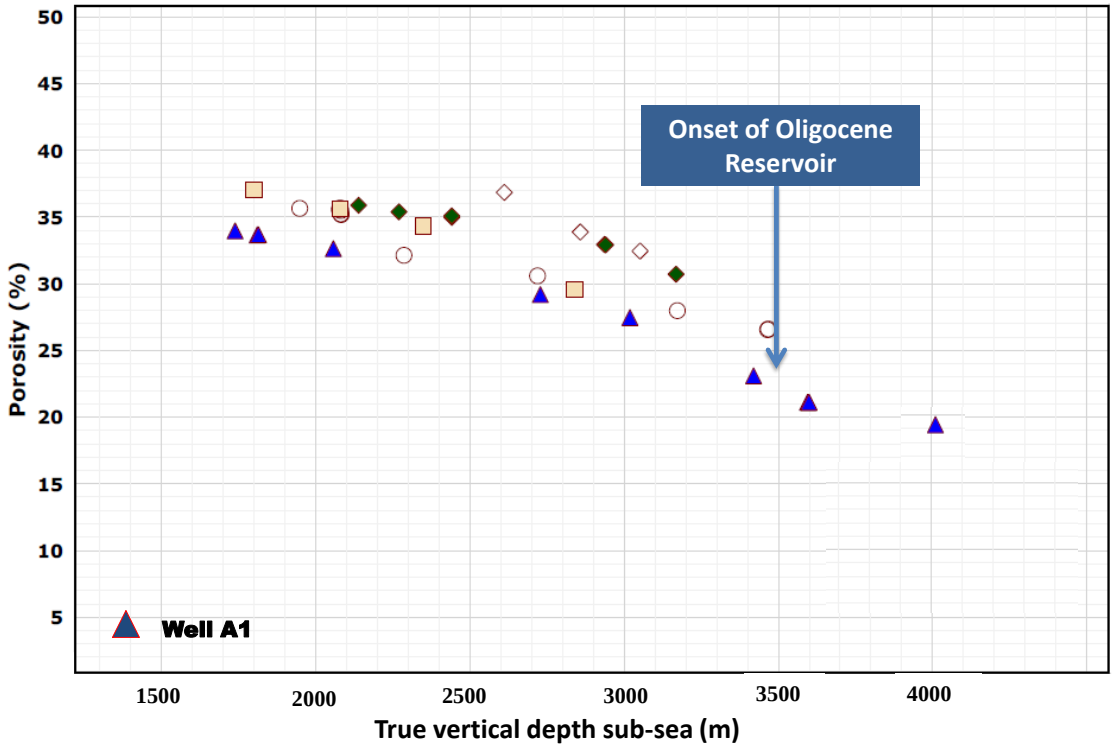

Fig. 14. Porosity-depth trend showing a reduction in porosity for several stacked reservoirs plotted against depth for 4 wells. Well A1, the deepest well, highlighted in blue triangles with Oligocene porosity starting at 3500m.

at the present day, which can explain the very minor quartz overgrowths observed in samples of this age. It is well established that overpressured reservoirs retain porosity because mechanical compaction is inhibited (Taylor et al. 2010).

The simulated pressure history of the reservoirs indicates that the Miocene reservoirs have not developed overpressure, but that the Oligocene rocks did encounter overpressure from the Middle Miocene, the overpressure value having continued to increase to the present day having a value of about 12 MPa, as seen from the separation of the modelled pore pressure (PP) and hydrostatic pressure (H) lines (Fig. 16b). Notwithstanding, the overpressured Oligocene sandstones are not likely to have avoided all quartz cementation because they were exposed to temperatures high enough for cementation from the Early Miocene (19 Ma), which is before the significant cementation in the Late Miocene (10 Ma): the temperature for quartz cementation was reached 9 Ma before overpressure developed.

Quartz cement modelling. By implementing the Walderhaug quartz cementation model as part of the simulation, the percentage pore space occluded by cement was estimated. The results show that cement volume tends to increase both with depth and up-dip (Fig. 6) as water column thickness decreases up-dip and mean overburden increases. Little or no cement is predicted above 3000 m in the area of Well 1A but cementation starts to develop from about 3450 m depth within the Lower Miocene reservoirs. In sandstones at this depth, less than 5% of the pore space has been occluded by quartz cement. The cement volume increases steadily with depth into the potential Oligocene reservoirs where values of close

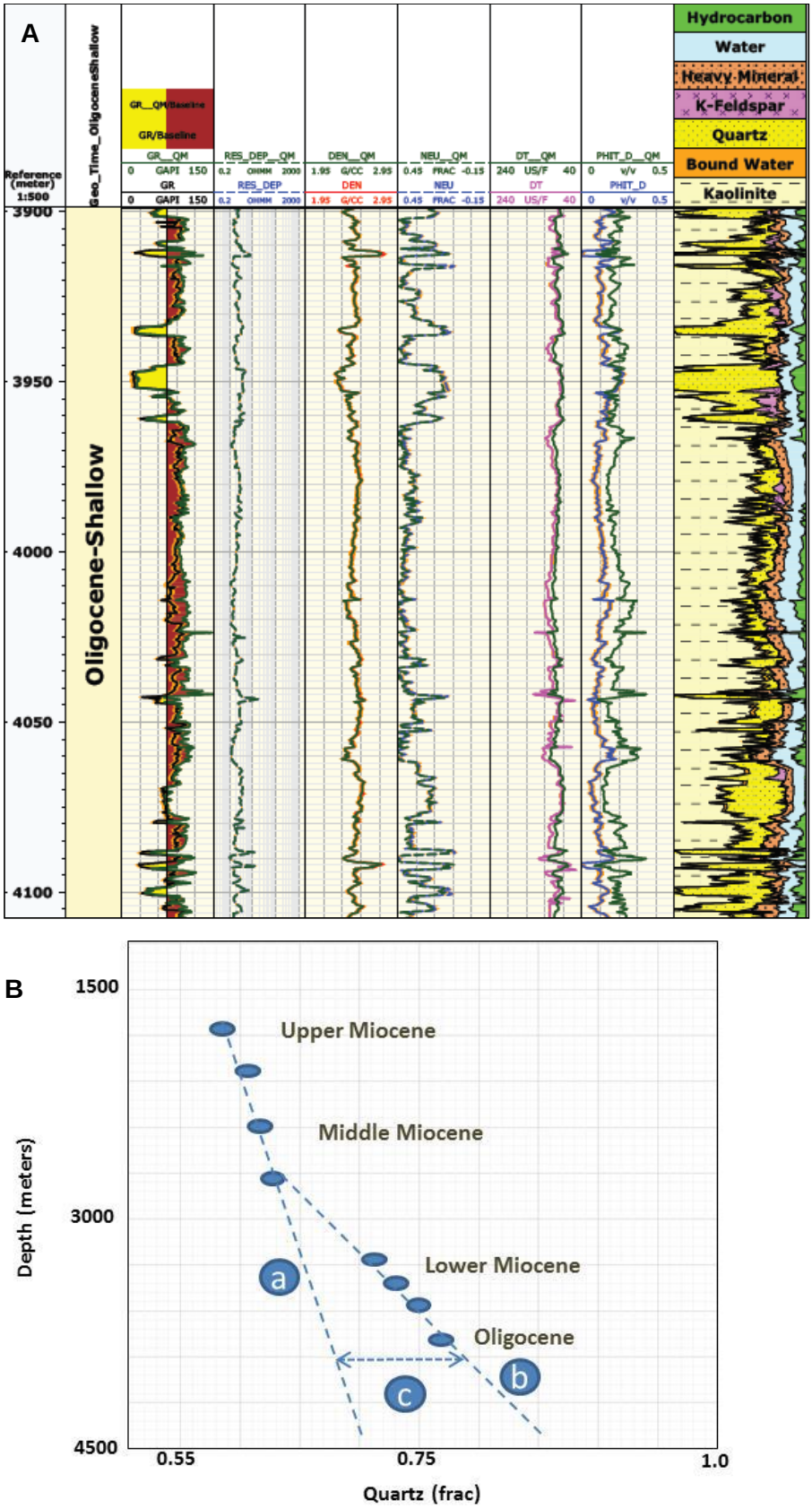

Fig. 12. (A) Modelled mineral volumes (quartz=yellow, feldspar=pink, mica=black, kaolinite= cream with dash).Columns 3is Gamma ray: 4 is resistivity; 5 is density; 6 is neutron and 7 is porosity. Logs with the suffix ELAN represent back calculated logs: (B) Cross plot of modelled quartz volume against depth.

to 14% occlusion of the pore space are reached. The minor quartz cement observed from the petrological study for the Lower Miocene reservoir and the absence of quartz in the Middle Miocene reservoir agrees with this simulated result. The simulated result is also displayed as a 1D extraction at the well location from the 2D model with cement volume plotted against depth (Fig. 7).

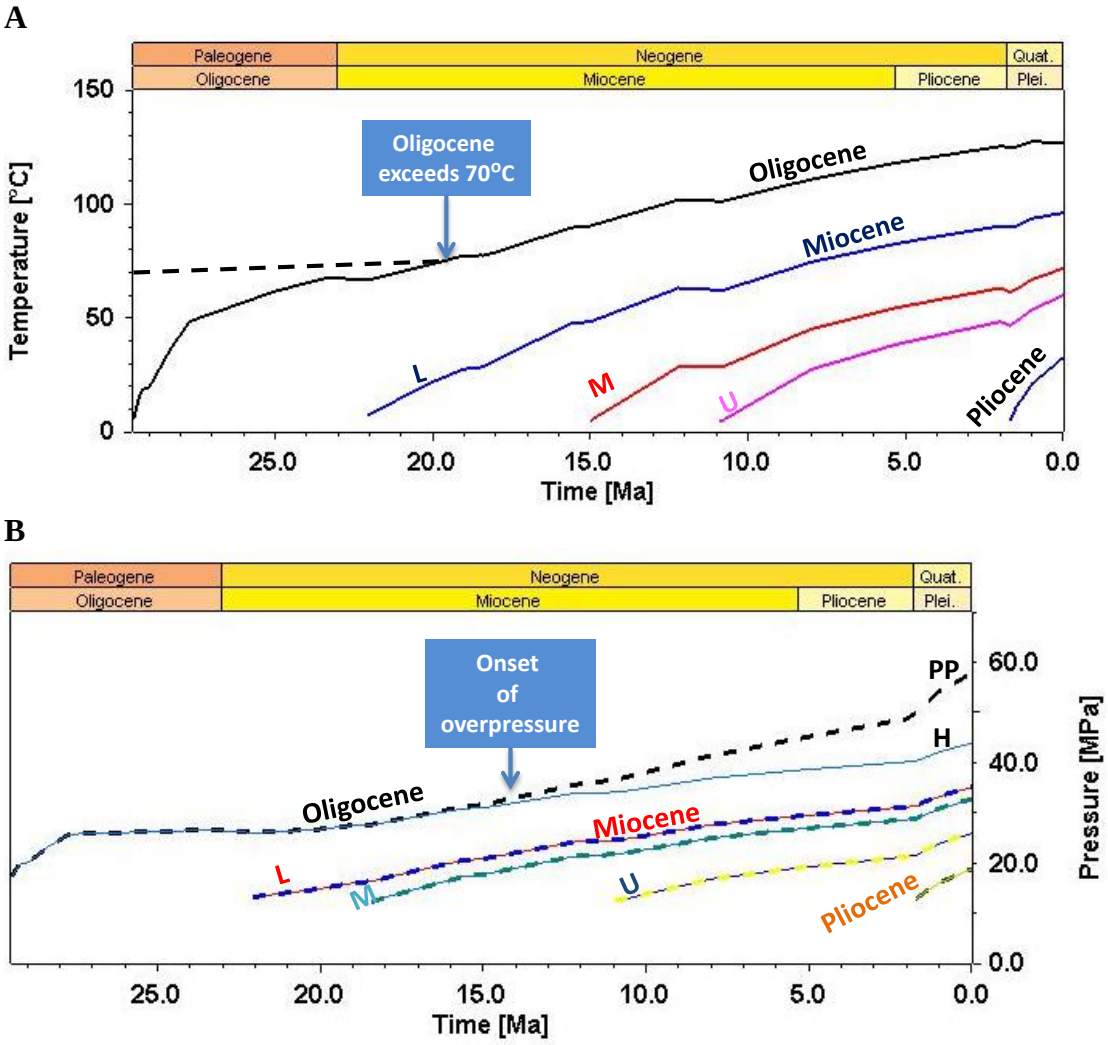

Fig. 16. Modelled thermal (A) and pressure (B) history. The pressure histories (B) are plotted for both hydrostatic (line) and pore pressure (dash): (L=Lower Miocene, M= Middle Miocene and U= Upper Miocene).

The trend observed in the quartz model also closely resembles the trend from the multimineral analysis of Figure 15b. A corresponding decrease in modelled porosity from Miocene to Oligocene reservoirs is seen when the modelled porosity is plotted against depth. A good match is seen between the modelled porosity and the average calculated porosity from the well log (Fig. 17).

A 1D column that was extracted from a 2D basin model near the deepest well shows the volume fraction of pore space filled with quartz cement plotted against depth (see Fig. 7). The figure shows an increase in cement with depth as is expected; a similar trend is

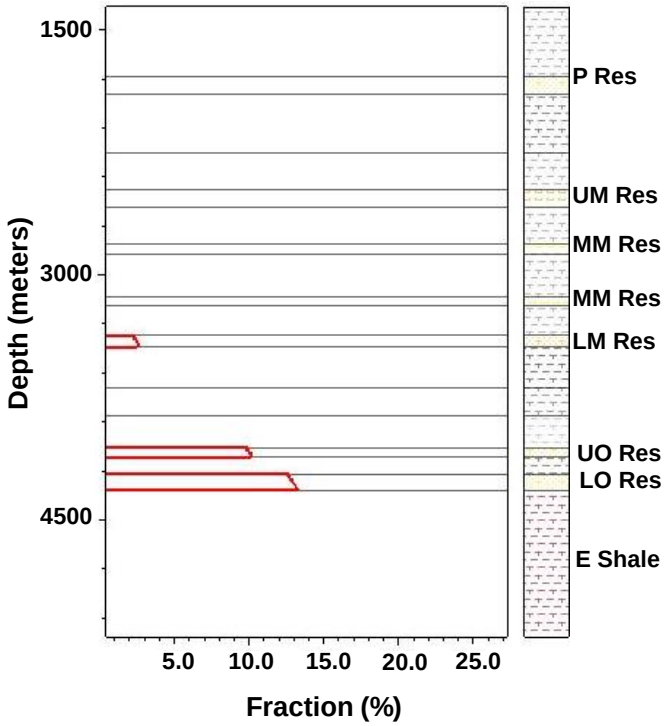

Fig. 16. Fraction of pore space occluded by quartz cement plotted against depth: a 1D extract from the 2D model in Fig. 11. (Res =reservoir, P =Pliocene, UM = Upper Miocene, MM = Mid-Miocene, LM = Lower Miocene, UO = Upper Oligocene, LO = Lower Oligocene, E = Eocene).

predicted from multimineral petrophysical evaluation, where major rock mineral volumes have been estimated from well log responses. A good match is seen between the original input log and the reverse calculated versions of the logs with a suffix of ELAN attached to the name of the curve (Fig. 15a). This is a good quality control for the estimated volumes of quartz, feldspar, zircon and kaolinite.

A cross plot of the fraction of quartz volume against depth shows an increase in quartz with depth. There is a clear demarcation of two trends, a higher gradient down to the Middle Miocene (trend a) and a gentler gradient from Lower Miocene down to the Oligocene (trend b). It is not possible to differentiate between detrital and authigenic quartz as contributors to the total quartz as indicated on this plot. However, if we assume a stable sediment supply yielding a constant quartz volume input, then trend a can be interpreted as a function of physical compaction due to the weight of the overburden, such that the quartz volume increases slowly and steadily as a percentage of the total rock volume. Whereas the second trend b shows a more rapid increase of quartz volume with depth, which can be interpreted as a function of both compaction and quartz volume increase due to cementation.
The separation of trends a and b, designated line c, can be assumed to be additional quartz volume of about 10% due to quartz cement. This assumption is supported by: (1) the modelled quartz cement that is based on the Walderhaug algorithm, which shows an onset of quartz cementation from the Lower Miocene, increasing volumetrically in the Oligocene to a quartz cement volume of less than 14% (Fig. 7); and (2) the presence of quartz overgrowths noted from the petrographic inspection of the Lower Miocene samples (Fig. 10d, e). No quartz cement was seen in samples from shallower or younger reservoirs.

Discussion

The focus of this work is to better understand the reservoir potential of the Oligocene interval buried below 3800 m – most importantly how, and to what extent, quartz cementation has reduced porosity below that attributable to the depositional character and mechanical compaction with burial. The burial-related mechanical compaction, temperature and pressure histories have been calculated by basin modelling and have then been used to calculate the probable amounts of quartz cementation throughout the burial history, given sediment properties such as quartz content and grain size, which are known to control cementation rate.

There is direct evidence of some quartz cementation at the lower Miocene. CL images of samples from the deepest cored Lower Miocene interval at 3450 m reveal the presence of syntaxial quartz overgrowths (Fig. 10d, e). However the overgrowth is less than 30 mm thick, suggesting that the effect on porosity here is likely to be minimal. This expectation is supported by the porosity calculated from density logs for this interval, which shows an average value of about 25% (Fig. 14). This value is consistent with only mechanical compaction. The presence of quartz overgrowths in the Lower Miocene is taken as indicative of an increase in cementation with depth and consequently the potential for a significant degree of quartz cementation within the Oligocene reservoir. There is, however, no direct evidence from the Oligocene, so quartz cementation calculations require a critical assessment of the assumed parameters.

The main parameters that control quartz cementation rate as calculated here are mineralogy, grain size and the degree of grain coating, together with temperature, pore fluid pressure (particularly its deviation from the hydrostatic pore pressure) and potentially the presence of petroleum. These are discussed below for the Oligocene, with recognition of the level to which the values are known.

Mineralogy

The Oligocene has not been sampled directly so we must make an estimate of the likely mineralogy on the basis of an assessment of the overlying Miocene succession. There is no reason to assume that sediment supply to the deep water varied significantly during this time interval, as the provenance and supply routes have not changed, so we can use values taken from the Miocene. This is true throughout the Miocene section, as well as into the Pliocene. The sandstone turbidite reservoirs of Miocene age are all quartz arenites (i.e.>90% quartz by weight). Assuming a depositional porosity of 40% by volume, we have calculated an initial volume percent of 54% quartz, which we have used in the quartz cementation calculations. There is a general absence of calcite and relatively low percentages of clay minerals, so we would not expect marked cementation or pore-clogging by other authigenic minerals.

Grain size

Following a similar reasoning and based on an average of the range of mean grain-size values found in Miocene reservoirs, we have assumed a value for the Oligocene sands of 0.12 mm, i.e. fine-grained sandstone. It is interesting to compare this with other turbidite reservoirs of similar age. In the Lower Congo Basin, for example, field data indicate that the

petroleum-bearing Oligocene reservoirs have grain sizes that vary from very fine to very coarse (0.125 –2 mm) (Dessus & Abreu 2002; Pelleau et al. 2002; Delattre et al. 2004). The Oligocene reservoirs of the Campos Basin are mostly medium to coarse-grained (0.25–1 mm) (Souza et al. 1989; Pinto et al. 2001; Bruhn et al. 2003). In our model calculations, different input grain sizes have a significant effect on calculated quartz cementation amount. A grain size of 0.05 mm (coarser silt) produced 19% of the pore volume filled with cement whereas a grain size of 2 mm (very coarse sand) produced a cement volume of 1.8%. It is possible that the Oligocene sands may have been deposited in a marginally more distal slope setting. Indeed there is evidence from our interpretation of depositional environments that the Oligocene reservoirs represent deposition in ponded mid-slope lobes whereas the Miocene reservoirs are inferred slope channel deposits (Chudi 2015). However, it is unlikely that the very slightly finer grain size of the Oligocene sandstones would make more than a 1–2% difference in the occlusion of porosity by quartz cementation.

Grain coating

In this study, the Miocene samples observed in SEM and under the optical microscope did not show any evidence of grain coating; this was true for all samples studied including those from the earliest Miocene. However, in order to assess the sensitivity to coating, we systematically increased the grain coating value in our model from 0% to 100%, and as coating percentage increased the calculated volume of quartz cement decreased steadily. Full (100%) grain coating (perhaps unsurprisingly) completely inhibits cementation, yielding no cement, whereas a complete absence of grain coating favours cementation, and yielded up to 14% occlusion of the pore space by cement. The evidence we have indicates that the latter figure is more likely to be representative of the Oligocene section.

Temperature

Temperature is calculated directly in the basin model as is pore pressure, together with its deviation from the hydrostatic pressure gradient. These values have been used to calculate the degree of quartz cementation. Sensitivity studies have also been performed around these values to accommodate reasonable variations either side of the basin simulation results. The heat flow history within this passive margin was modelled using the McKenzie heat flow model, with peak heat flow of 110 mW/m^2 reached during rifting (at 100 Ma) and gradually dropping to a present day 53mW/m^2. This choice of heat flux over the basin evolution resulted in a cement volume of just below 14% of the available pore space. When synrift heat flow values between 65 and 110 mW/m^2 (Allen and Allen 1990) were used in the basin model, the calculated cement volume remained effectively unchanged, presumably because the conditions for cementation had not been reached in the reservoir rocks. However, when the heat flow was altered during the Miocene, the presumed time of quartz cementation onset, the calculated cement pore volume was significantly affected. Using a Miocene heat flow 35 mW/m^2 produces low cementation (<8%) whereas a higher heat flow of 65 mW/m^2 yielded relatively higher cementation (up to 17%). This is to be expected as effectively the time of onset of cementation is being changed.

Neither a variable peak heat flow nor a Miocene variation is justified geologically and basin models that incorporate these heat flows do not produce values that match the measured present-day temperature or vitrinite data. Nevertheless, these calculations are a good

illustration of the significant impact of heat flow on quartz diagenesis where a change in heat flow value is justified.

Onset temperature for quartz cementation

The onset temperature of quartz cementation has been reported to be between 708C and 135C (Walderhaug 1994; Walderhaug 2000; Worden & Morad 2009; Taylor et al. 2010). The bulk of the literature suggests values closer to the lower end of this range for significant onset. Many of the models also have no lower cut-off temperature, but simply infer that reaction rates will be so low as to have no noticeable effect. For this study, we have taken the lower end of this range, i.e. 70^{o}C, as the temperature for the onset of quartz precipitation in order to model the maximum likely adverse effect on potential reservoir properties. The Upper and Middle Miocene has no evidence of quartz cementation, which is commensurate with its low formation temperature throughout its burial history. The Lower Miocene section shows a low volume of quartz cement (average of less than 5% of the pore space) in the study area, which can be attributed to the shallow burial depth of the sediments (800–1300 m) with a temperature that has just entered the window for the onset of quartz cementation. However, the Oligocene section is buried at depths greater than 3800 m and has therefore experienced temperatures exceeding 70^{o}C for a longer time period. Our models show up to 14% of the pore space has suffered quartz cementation. We therefore suggest that our results, both observation and modelling, support the case for the onset of quartz cementation at the low end of the published temperature range.

Pressure

The Middle and Lower Miocene reservoirs do not develop overpressure in the 2D basin model but the Oligocene reservoirs do develop overpressure starting in the Middle Miocene (14 Ma) and continuing to increase up to the present day. Overpressure is typically expected to result in reduced cementation as compared with the hydrostatic equivalent. An in-depth investigation of the effect of overpressure development on cementation is beyond the, scope of this study, but generally overpressure can be thought of as a fluid pressure state that is representative of a deeper location but at a lower temperature than would normally be associated with that deeper location. Here the model shows that the Oligocene reservoir becomes overpressured at 14 Ma, which is about 6 Ma after the conditions for cementation have been reached. If correct, earlier cementation would not have been affected by overpressure but later cementation may well have been impeded.

Hydrocarbons

Oil charge is another potential influence on cementation, although the effectiveness of petroleum in reducing the cementation rate, or stopping it completely, is widely debated (Marchand et al. 2002; Wilkinson et al. 2004; Taylor et al. 2010). Hydrocarbon coating agents were observed during SEM analysis of the Middle Miocene samples and dead oil was observed coating grains (Fig. 11). Considering that early oil emplacement can halt or reduce quartz cement precipitation (Taylor et al. 2010), it is therefore possible that the presence of this oil seen only in the Middle Miocene samples may have helped in preserving the porosity.

Comparative Oligocene reservoirs. Here we briefly compare the potential Oligocene reservoirs of the Niger Delta that we have studied with two other Oligocene turbidite

systems along the South Atlantic Margin: (1) the Lower Congo Basin, offshore Angola, and (2) the Campos Basin, offshore SE Brazil. The quality of the reservoirs and the corresponding key controlling factors are of primary importance.

The Lower Congo Basin is one of several different sub-basins developed along the West African passive margin, and is one of the most prolific, with major discoveries made within both Oligocene and Miocene turbidite systems of the Malembo Formation (Broucke et al. 2004). The most significant discoveries have been made in the Oligocene section, most notably the Girassol field, which has oil in place estimated at 1550 mmbbl and recoverable reserves placed at 725 mmbbl trapped within Oligocene turbidite channel–levee complexes. The field is located within a water depth of 1350–1450 m (Pelleau et al. 2002).

Whereas the Oligocene sediments of the Niger Delta slope system are found at depths greater than 3800 m below sea-level (up to 3000 m below the seafloor), the Oligocene reservoirs in Girassol field are located at a depth of 2400 m below sea-level (around 1000 m below the seafloor). The lower Congo Oligocene reservoirs have therefore undergone less burial and compaction. This is reflected in the wholly unconsolidated nature of the fine to very coarse sands, which exhibit excellent reservoir quality, having porosities of up to 40% and permeabilities greater than 5D. The Congo Basin reservoirs are also normally pressured with present-day temperatures of 58–69^{o}C (Dessus & Abreu 2002; Pelleau et al. 2002; Delattre et al. 2004). The regional geology of the area does not suggest that the Malembo Formation has at any time been exposed to any physiochemical conditions that would have led to the precipitation of any significant porosity-occluding diagenetic minerals, such as early quartz or calcite cements (Broucke et al. 2004; Gay et al. 2006).

Conjugate to the basins in West Africa is the Campos Basin of the Brazilian margin that lies beneath the coastal plain, continental shelf and slope along the western South Atlantic Ocean. The Campos Basin is the most prolific of the twelve east Brazilian offshore basins. (Bruhn et al. 2003). Turbidites constitute the main reservoir play in the Campos Basin, representing 37 different oilfields, including the Marlim Complex super giant field, which encompasses the Marlim Field itself and the surrounding fields of East Marlim, West Marlim and South Marlim (Souza et al. 1989; Bruhn et al. 2003). The total estimated oil in place for the Marlim Complex is about 13.9 billion barrels of oil, with the Marlim field itself accounting for over 57% of the total volume of hydrocarbon (Souza et al. 1989). The principal reservoir of the Marlin field is the Oligocene Carapebus Member of the Campos Formation. The Marlim field was discovered by the first exploratory well drilled at a water depth of about 850 m. The Oligocene reservoirs, located at a depth of about 2700 m below sea-level (i.e. >2000 m below the seafloor), are known for three outstanding qualities: (1) predictability from seismic data, (2) good hydraulic connectivity, and (3) excellent petrophysical properties. Reservoir average porosities and permeabilities typically range between 27% and 30%, and 1000–2000 mD respectively (Pinto et al. 2001).

The sand-rich reservoirs of the Marlim field comprise turbidite lobes, which accumulated in wide intraslope depressions. The reservoir facies comprise mostly amalgamated graded beds of medium to very fine grained sandstones that are poorly consolidated, poorly sorted and have a low volume of silt, clay and diagenetic minerals. The low degree of cementation in the Oligocene reservoirs is attributed to the following factors (Moraes 1989; Soldan et al.

1995): (1) reservoir temperatures of about 80C today and hence short residence times within the quartz-cementation window, (2) early oil emplacement that has inhibited cementation, (3) early carbonate cementation that persisted to depth and inhibited pressure dissolution, and (4) late-stage carbonate dissolution and creation of secondary porosity.

Conclusions

(1) The potential Niger Delta Oligocene reservoir of the study area is interpreted to have been subjected to temperatures at or above 70°C from the Early Miocene to the present day. Our use of this temperature as the starting temperature for the onset of quartz precipitation is validated by the observation and modelling results presented.
(2) Petrological and petrophysical analyses of quartz in the Lower Miocene suggest an increase in quartz overgrowth volume with depth, indicating that the Oligocene sediments are likely to be cemented.
(3) The possible volume of pore space occluded by cement in the Oligocene has been predicted to be (just) less than 14% of the available pore space.
(4) Despite both modelled results and inferences suggesting the possibility of quartz cementation in the potential Oligocene reservoir, the quartz cement volume predicted from 2D simulations is not sufficient to prevent the Oligocene interval of the Agbada Formation from being a viable hydrocarbon reservoir.
(5) The properties of comparable Oligocene reservoirs from the Lower Congo Basin and Campos Basin are more similar to the reservoir properties of the Miocene turbidites of the Niger Delta that have been buried to a depth range of 2400–3000 m than those of the Oligocene system. It is very likely that one of the principal factors controlling reservoir quality is the depth of burial and the associated physiochemical conditions, since the best quality reservoirs are seen at depths of less than 3000 m below sea-level in all three basins.
(6) Temperature-induced physicochemical factors that favour quartz cementation are prevalent in sandstones that are buried deeper than 3000 m within the Niger Delta deepwater system. The potential Oligocene reservoirs are currently located at depths >3800 m below sea-level.
(7) Modelling carried out in this study suggest that reservoir properties of the Oligocene turbidite sands of the Niger Delta slope system are only slightly reduced from those of the Miocene (up to 14% porosity occlusion). They therefore represent a very viable future exploration target.
(8) We suggest that this integrated approach using petrological, petrophysical and basin modelling is an important and novel methodology with widespread applicability to more accurate prediction of sandstone reservoir quality in the subsurface.

We wish to express our appreciation to Shell in Nigeria and The Hague for providing the data and particularly to Daniel Agbaire of Shell Nigeria and Andy Bell of Shell Global Solutions International, The Hague, for their expert advice. Also special thanks to Thomas Hantschel, Daniel Palmowski and Nour Koronful of Schlumberger Aachen for allowing the use of PetroMod software and for all the technical discussions, which have considerably enhanced this work. The authors are extremely grateful to the reviewers of this article for their copious efforts. This project is part of Obinna Chudi's PhD, which has been generously sponsored by the Petroleum Technology Development Fund (PTDF), Nigeria.

References

Ajdukiewicz, J.M. & Larese, R.E. 2012. How clay grain coats inhibit quartz cement and preserve porosity in deeply buried sandstones: observations and experiments. AAPG Bulletin, 96, 2091–2119.

Allen, P.A. & Allen, J.R. 1990. Basin Analysis: Principles and Applications. Blackwell Scientific Publications, Oxford.

Athy, L.F. 1930. Density, porosity, and compaction of sedimentary rocks. Bulletin of the American Association of Petroleum Geologists, 14, 1–24.

Bilotti, F. & Shaw, J.H. 2005. Deep-water Niger Delta fold and thrust belt modeled as a critical-taper wedge: the influence of elevated basal fluid pressure on structural styles. AAPG Bulletin, 89, 1475–1491.

Bjørkum, P.A., Oelkers, E.H., Nadeau, P.H., Walderhaug, O. & Murphy, W.M. 1998. Porosity prediction in quartzose sandstones as a function of time, temperature, depth, stylolite frequency, and hydrocarbon saturation. AAPG Bulletin, 82, 637.

Bloch, S., Lander, R.H. & Bonnell, L. 2002. Anomalously high porosity and permeability in deeply buried sandstone reservoirs: origin and predictability. AAPG Bulletin, 86, 301–328.

Briggs, S.E., Cartwright, J. & Davies, R.J. 2009. Crustal structure of the deepwater west Niger Delta passive margin from the interpretation of seismic reflection data. Marine and Petroleum Geology, 26, 936–950.

Broucke, O., Temple, F., Rouby, D., Robin, C., Calassou, S., Nalpas, T. & Guillocheau, F. 2004. The role of deformation processes on the geometry of mud-dominated turbiditic systems, Oligocene and Lower–Middle Miocene of the Lower Congo basin (West African Margin). Marine and Petroleum Geology, 21, 327–348.

Bruhn, C.H., Gomes, J.A.T., Lucchese, J.R.C. & Johann, P.R. 2003. Campos Basin: reservoir characterization & management–Historical overview & future challenges. Paper presented at the Offshore Technology Conference, 5–8 May 2003, Houston, 5–8.

Chudi, O.K. 2015. Predicting Oligocene reservoir potential in the deep-water Western Niger Delta: an integrated basin modelling and diagenetic study. PhD thesis, Heriot-Watt University.

Corredor, F., Shaw, J.H. & Bilotti, F. 2005. Structural styles in the deep-water fold and thrust belts of the Niger Delta. AAPG Bulletin, 89, 753–780.

Damuth, J.E. 1994. Neogene gravity tectonics and depositional processes on the deep Niger Delta continental margin. Marine and Petroleum Geology, 11, 320–346.

Delattre, E., Authier, J.F., Rodot, F., Petit, G. & Alfenore, J. 2004. Review of sand control results and performance on a deep water development-A case study from the Girassol Field Angola. Paper presented at the SPE Annual Technical Conference and Exhibition, 26–29 September 2004, Houston, TX.

Deptuck, M.E., Sylvester, Z., Pirmez, C. & O'Byrne, C. 2007. Migration–aggradation history and 3-D seismic geomorphology of submarine channels in the Pleistocene Benin-major Canyon, western Niger Delta slope. Marine and Petroleum Geology, 24, 406–433.

Derks, J., Swientek, O., Fuchs, T., Kauerauf, A., Al-Quattan, M. & Al-Saeed, M. 2012. Three-Dimensional Basin and Petroleum System Model of the Cretaceous Burgan Formation, Kuwait: Model-in-Model, High-Resolution Charge Modeling. Basin Modeling. New Horizons in Research and Applications, AAPG Hedberg Series, 4, 159.

Dessus, J.L. & Abreu, J. 2002. Girassol: drilling and completion experience gained through first 12 wells. Offshore Technology Conference, 6–9 May, Houston, Texas, 14168, 6–9.

Doust, H. & Omatsola, E. 1990. Niger Delta. In: Edwards, J.D. & Santogrossi, P.A. (eds), Divergent/Passive Margin Basins. American Association of Petroleum Geologists, 48, 201–238.
Dowey, P.J., Hodgson, D.M. & Worden, R.H. 2012. Prerequisites, processes and prediction of chlorite grain coatings in petroleum reservoirs: a review of subsurface examples. Marine & Petroleum Geology, 32, 63–75.
Ejedawe, J., Coker, S., Lambert-Aikhionbare, D., Alofe, K. & Adoh, F. 1984. Evolution of oil-generative window and oil and gas occurrence in Tertiary Niger Delta Basin. Bulletin of the American Association of Petroleum Geologists, 68, 1744–1751.
Evamy, B.D., Haremboure, J., Kamerling, P., Knaap, W.A., Molly, F.A. & Rowlands, P.H. 1978. Hydrocarbon habitat of Tertiary Niger Delta. American Association of Petroleum Geologists Bulletin, 62, 1–39.
Evans, J., Hogg, A.J., Hopkins, M.S. & Howarth, R.J. 1994. Quantification of quartz cements using combined SEM, CL, and image analysis. Journal of Sedimentary Research, 64.
Gay, A., Lopez, M., Cochonat, P., Se´ranne, M., Levache´, D. & Sermondadaz, G. 2006. Isolated seafloor pockmarks linked to BSRs, fluid chimneys, polygonal faults and stacked Oligocene–Miocene turbiditic palaeochannels in the Lower Congo Basin. Marine Geology, 226, 25–40.
Gier, S., Worden, R.H., Johns, W.D. & Kurzweil, H. 2008. Diagenesis and reservoir quality of Miocene sandstones in the Vienna Basin, Austria. Marine and Petroleum Geology, 25, 681–695.
Haack, R.C., Sundararaman, P., Diedjomahor, J.O., Xiao, H., Gant, N.J., May, E.D. & Kelsch, K. 2000. Chapter 16: Niger delta petroleum systems, Nigeria. In: Mello, M.R. & Katz, B.J. (eds) Petroleum Systems of South Atlantic Margins. American Association of Petroleum Geologists, Memoir, 73, 213–231.
Hermanrud, C. 1993. Basin modelling techniques-an overview. In Basin Modelling: Advances and Applications. Norwegian Petroleum Society, Special Publications, 3, 1–34.
Lambert-Aikhionbare, D. & Ibe, A. 1984. Petroleum source-bed evaluation of Tertiary Niger delta: discussion. Bulletin of the American Association of Petroleum Geologists, 68, 387–389.
Lander, R.H. & Walderhaug, O. 1999. Predicting porosity through simulating sandstone compaction and quartz cementation. AAPG Bulletin, 83, 433–449.
Marchand, A.M., Smalley, P.C., Haszeldine, R.S. & Fallick, A.E. 2002. Note on the importance of hydrocarbon fill for reservoir quality prediction in sandstones. AAPG Bulletin, 86, 1561–1572.
McBride, E.F. 1963. A classification of common sandstones. Journal of Sedimentary Research, 33.
Moraes, M.A. 1989. Diagenetic evolution of Cretaceous- Tertiary turbidite reservoirs, Campos Basin, Brazil. AAPG Bulletin, 73, 598–612.
Nwachukwu, S. 1976. Approximate geothermal gradients in Niger Delta Sedimentary Basin. AAPG Bulletin, 60, 1073–1077.
Pelleau, R., Serceau, A. & Total Fina Elf. 2002. The Girassol development: project challenges.
Peters, K.E., Moldowan, J.M., Mccaffrey, M.A. & Fago, F.J. 1996. Selective biodegradation of extended hopanes to 25-norhopanes in petroleum reservoirs. Insights from molecular mechanics. Organic Geochemistry, 24, 765–783.
Pinto, C., Antonio, C., Guedes, S.S., Bruhn, C.H., Gomes, J.A.T. & Netto, J. 2001. Marlim complex development: a reservoir engineering overview. Paper presented at the SPE Latin

American & Caribbean Petroleum Engineering Conference, Buenos Aires, Argentina, 25–28 March 2001.
Reijers, T. 2011. Stratigraphy and sedimentology of the Niger Delta. Geologos, 17.
Saugy, L. & Eyer, J.A. 2003. Fifty years of exploration in the Niger Delta (West Africa). In: Halbouty, M.T. (ed.) Giant Oil and Gas Fields of the Decade 1990–1999. AAPG Memoirs, 78, 211–226.
Siever, R. 1983. Burial history and diagenetic reaction kinetics. AAPG Bulletin, 67, 684–691.
Short, K. & Stauble, A. 1967. Outline of geology of Niger Delta. Bulletin of the American Association of Petroleum Geologists, 51, 761–779.
Sneider, R.M. 1990. Reservoir Description of Sandstones. Sandstone Petroleum Reservoirs. Springer, New York.
Soldan, A., Cerqueira, J., Ferreira, J., Trindade, L., Scarton, J. & Cora´, C. 1995. Giant Deep Water Oil Fields in Campos Basin, Brazil: a Geochemical Approach. Revista Latino-Americana de Geoquimica Organica, 1, 14–27.
Sombra, C.L. & Chang, H.K. 1997. Burial history & porosity evolution of Brazilian Upper Jurassic to Tertiary sandstone reservoirs. In: Kupecz, J.A., Gluyas, J. & Bloch, S. (eds) Reservoir Quality Prediction in Sandstones and Carbonates. AAPG Memoir, 69, 79–89.
Sonde, A., Omobude, O., Chudi, O., Oghene, U. & Coker, T. 2011. Integrated 3D modelling in a structurally complex brown field: a foundation for improved reservoir management and optimisation of further development. Nigeria Annual International Conference and Exhibition, 2011. Society of Petroleum Engineers.
Souza, J., Scarton, J., Candido, A., Cruz, C. & Cora, C. 1989. The Marlim & Albacora Fields: geophysical geological & reservoir aspects. Paper presented at the
Offshore Technology Conference, Houston TX, 1–4 May 1989.
Talc¸in, M.N. 1991. Basin modeling and hydrocarbon exploration. Journal of Petroleum Science and Engineering, 5, 379–398.
Taylor, T.R., Giles, M.R. et al. 2010. Sandstone diagenesis and reservoir quality prediction: models, myths, and reality. AAPG Bulletin, 94, 1093–1132.
Tuttle, M.L., Charpentier, R.R. & Brownfield, M.E. 1999. The Niger Delta Petroleum System: Niger Delta Province, Nigeria, Cameroon, and Equatorial Guinea, Africa. US Department of the Interior, US Geological Survey Open-File Report 99-50-H.
Underdown, R. & Redfern, J. 2008. Petroleum generation and migration in the Ghadames Basin, north Africa: a two-dimensional basin-modeling study. AAPG Bulletin, 92, 53–76.
Walderhaug, O. 1994. Precipitation rates for quartz cement in sandstones determined by fluid-inclusion microthermometry and temperature-history modeling. Journal of Sedimentary Research, 64, 324–333.
Walderhaug, O. 2000. Modeling quartz cementation and porosity in Middle Jurassic Brent Group sandstones of the Kvitebjørn field, northern North Sea. AAPG Bulletin, 84, 1325–1339.
Weber, K. 1971. Sedimentological aspects of oil fields in the Niger Delta. Geologie en Mijnbouw, 50, 559–576. Welte, D. & Yalcin, M. 1988. Basin modelling – a new comprehensive method in petroleum geology. Organic Geochemistry, 13, 141–151.
Whiteman, A. 1982. Nigeria: Its Petroleum Geology, Resources & Potential. Vol. 1. Springer, Netherlands.
Wilkinson, M., Haszeldine, R.S., Ellam, R.M. & Fallick, A. 2004. Hydrocarbon filling history from diagenetic evidence: Brent Group, UK North Sea. Marine and Petroleum Geology, 21, 443–455.

Worden, R.&Morad, S. 2009. Quartz cementation in oilfield sandstones: a review of the key controversies. In: Worden, R. & Morad, S. (eds) Quartz Cementation in Sandstones. Blackwell Publishing Ltd, Oxford,29, 1–20.
Wygrala, B. 1988. Integrated computer-aided basin modelling applied to analysis of hydrocarbon generation history in a Northern Italian oil field. Organic Geochemistry, 13, 187–197.